



Original Research

Simulation of Delta and Omicron Variants Detection Using Surface Plasmon Resonance Based on Kretschmann-Raether Configuration

DiviyaDevi Paramasivam¹, Siti Aisyah Mualif^{1,2,3*}, Norhana Jusoh^{1,3}, Mariaulpa Sahalan^{1,2}, Nurul Atiqah Maaruf¹, Seri Mirianti Ishar⁴, Ahmad Razali Ishak⁵, and Mohd Yumaidie Aziz⁶

¹ Biomedical Engineering & Health Sciences Department, Faculty of Electrical Engineering, Universiti Teknologi Malaysia, 81310 UTM Johor, Malaysia

² Advanced Diagnostics and Progressive Human Care, Biomedical Engineering & Health Sciences Department, Faculty of Electrical Engineering, Universiti Teknologi Malaysia, 81310 UTM Johor, Malaysia

³ Medical Devices and Technology Centre, Universiti Teknologi Malaysia, 81310 UTM Johor, Malaysia

⁴ Forensic Science Program, Faculty of Health Sciences, Universiti Kebangsaan Malaysia, 43600 Bangi, Malaysia

⁵ Center for Environmental Health & Safety, Faculty of Health Sciences, Universiti Teknologi MARA, Puncak Alam Campus, 42300 Kuala Selangor

⁶ Department of Toxicology, Advanced Medical & Dental Institute, Universiti Sains Malaysia, 13200 Kepala Batas, Penang, Malaysia

ARTICLE INFO

Article History:

Received 29 May 2023

Accepted 29 May 2023

Available online 30 May 2023

Keywords:

COVID-19,
SARS-CoV-2,
Surface Plasmon Resonance,
Simulation,
Sensor

ABSTRACT

COVID-19 caused by SARS-CoV-2 has been mutated and emerged into different types of variants. Delta and Omicron variants remained as variants of concern as the Delta variant severely infects the unvaccinated individual, while the Omicron variant is the dominant variant circulating globally. Therefore, it is vital to identify these variants by developing a simpler method that detects both variants based on the antibody-antigen interactions. The Surface Plasmon Resonance (SPR) sensor based on the Kretschmann-Raether configuration provides label-free detection of SARS-CoV-2 variants by the antibody-antigen interaction. However, to date, there is no multiple SARS-CoV-2 variants detection methods have been implemented using SPR sensors based on the Kretschmann-Raether configuration. Therefore, this study is carried out to design an SPR sensor based on the Kretschmann-Raether configuration and to simulate the detection of these variants by this sensor using COMSOL Multiphysics software. In this study, an SPR sensor was designed with two detecting cells named Cell 1 and Cell 2, where each cell contains a 2E8 monoclonal antibody and COV2-06 monoclonal antibody respectively. The results show that the designed SPR sensor can distinguish and detect the Delta and Omicron variant successfully based on the antibody-antigen interaction with the sensitivities of $3.3968 \text{ deg RIU}^{-1}$ for Cell 1 and $4.5803 \text{ deg RIU}^{-1}$ for Cell 2. Therefore, this SPR sensor based on the Kretschmann-Raether configuration could be a potential alternative tool for currently available multiple SARS-CoV-2 variants detection methods as it provides label-free detection that is based on antigen-antibody interaction.

INTRODUCTION

Over the course of the pandemic, different variants of SARS-CoV-2 have been identified by the World Health Organization (WHO). Among the existing variants, SARS-CoV-2 Delta and Omicron variants are classified as Variants of Concern (VOCs).

Omicron variant is found capable of spreading easily and infects people regardless of vaccination status. As of now, a lot of detection methods have been developed to detect COVID-19, but only a few are applicable for multiple SARS-CoV-2 variants detection. Genomic sequencing is the sole method to determine variants of SARS-CoV-2. This method requires specialized equipment, costly and time-consuming (Xi et al., 2021). To date, there are no alternatives that do not require deoxyribonucleic acid (DNA) or nucleic acid amplification to detect multiple

* Siti Aisyah Mualif (aisyahmualif@utm.my)

Advanced Diagnostics and Progressive Human Care, Biomedical Engineering & Health Sciences Department, Faculty of Electrical Engineering, Universiti Teknologi Malaysia, 81310 UTM Johor, Malaysia

SARS-CoV-2 variants that infect the patients (Puligedda et al., 2021).

Surface plasmon resonance (SPR) sensor is one of the types of plasmonic biosensors that provides label-free detection of viruses by the means of antibody- antigen interaction (Puligedda et al., 2021). Currently, a lot of research has been carried out on the usage of SPR with different coupling methods such as optical fiber, grating coupler, waveguide coupler, and prism coupler to detect the SARS- CoV-2 virus (Asghari et al., 2021). Among these, the prism coupling method can be useful in the trial of developing SPR sensors for COVID-19 detection as it is the standard configuration that is based on the Kretschmann-Raether configuration (Asghari et al., 2021).

Therefore, in this study, a SPR sensor based on the Kretschmann-Raether Configuration is designed to simulate the Delta and Omicron variants detection using COMSOL Multiphysics software. This software uses the finite element method (FEM) with adaptive meshing and error control to simulate the Delta and Omicron variants detection using SPR sensor. Hence, provides an approximation of the real solution as a result where reflectivity curves will be produced as the result of the simulation of variants detection. In addition, features like parameter sweeps were used during simulation to get the desired result at an expected range of the parameters. Therefore, this software allows solving or processing of any phenomena that are related to different studies and this is suitable to be used in this study that is related to physics and chemistry.

MATERIALS AND METHOD

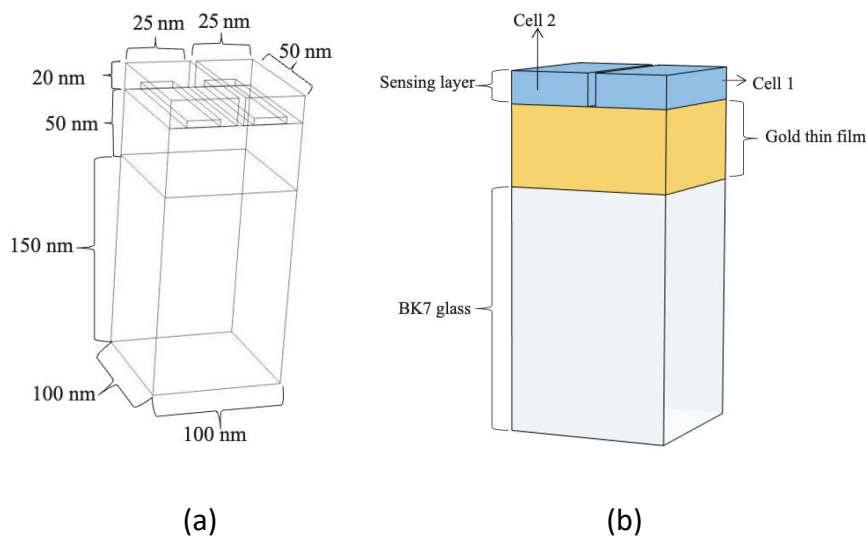
Designing the SPR sensor based on the Kretschmann-Raether Configuration to Detect the Delta and Omicron Variants

For designing the SPR sensor based on the Kretschmann-Raether configuration, the wave optics module, and the Electromagnetic Waves, Frequency Domain study were chosen in the COMSOL Multiphysics software. The dimension for each layer of the sensor was defined in the parameters under the global definition in the software. It is as depicted in the Figure 1. Table 1 shows the dimension defined for each layer in the

software. The diameter of gold (Au) was set at 50 nm to enable the evanescent field to excite the surface plasmon (Wang and Fan, 2016).

Table 1. Dimension for each layer

Name	Expression	Description
w	100[nm]	Sensor width
d	100[nm]	Sensor depth
t_{prism}	150[nm]	Thickness of glass layer
t_{gold}	50[nm]	Thickness of gold layer
t_{sl}	20[nm]	Thickness of sensing layer
$c1_h$	50[nm]	Height of Cell 1
$c1_w$	100[nm]	Width of Cell 1
$c1_d$	25[nm]	Depth of Cell 1
$c2_h$	50[nm]	Height of Cell 2
$c2_w$	100[nm]	Width of Cell 2
$c2_d$	25[nm]	Depth of Cell 2



The refractive indices for the Au and the BK7 prism layers were set (Mostufa et al., 2021; Das et al., 2020) during the simulation. After that, the 2E8 mAb and the COV2-06 mAb layers were added to Cell 1 and Cell 2 respectively by defining their dimension, refractive indices, concentration, and the chemical equations. Table 2 shows the dimensions, concentration, and refractive indices of 2E8 mAb and COV2-06 mAb. The concentrations of monoclonal antibodies were used because both 2E8 mAb and the COV2-06 mAb show higher binding responses to the spike RBD of the Delta and Omicron variants respectively (Ku et al., 2021; Puligedda et al., 2021).

Fig. 1 (a) Dimension for each layer and **(b)** SPR sensor designed using COMSOL Multiphysics software.

Table 2. Dimension, concentrations, and refractive indices of monoclonal antibodies

Cells	Dimension[nm]	Concentrations [nM]	Refractive indices
1 (2E8 mAb)	5x100x25 (Barrios, 2021)	1.23 (Puligedda et al., 2021)	1.3689 (Puligedda et al.,2021)
2 (COV2-06 mAb)		1.74 (Ku et al.,2021)	1.3358 (Mostufa et al.,2021)

The Floquet periodic boundary conditions (FPBC) were imposed on all plane boundaries along the z-axis of the structure to satisfy the “semi-infinite” condition for the excitation of surface plasmon as shown in Figure 2(a). This condition assumes that the SPR model is infinitely large, and the designed unit cell is repeating periodically in the plane of the gold thin film (Dormeny et al., 2020).

The ports for the SPR model were selected. The active port which is also known as the input port was imposed on the bottom surface of the BK7 prism as shown in Figure 2(b). For both Cell 1 and Cell 2, the input ports were the same and were named Port 1. The input port is significant because it is where the incident light is subjected at. At the resonance condition, the wave vector of the incident light matches the wave vector of the electrons oscillating on the gold metal surface (Michel et al., 2017). The output ports for Cell 1 and Cell 2 were selected separately as shown in Figure 2(c) and Figure 2(d) respectively.

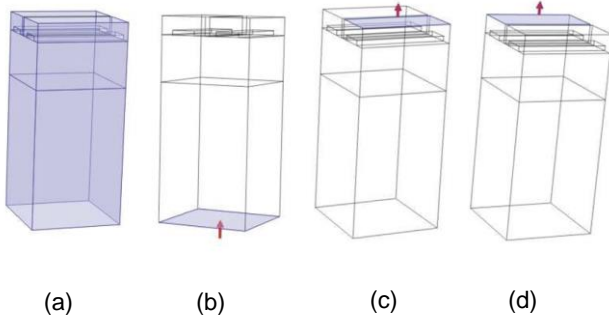


Fig. 2 (a) Periodic boundary conditions on all surfaces of the SPR sensor model, **(b)** Input port, Output port for **(c)** cell 1, and **(d)** cell 2.

Setting Mesh

For mesh, the automatic setting was chosen instead of the manual as it set the accurate minimum value and maximum value. The maximum and minimum values of mesh are 0.12660 and 0.0037970 respectively. This was done to decrease the time of simulation, memory requirement by controlling the number, type, and quality of elements. This creates an efficient and accurate simulation (Uddin et al., 2020). For this study, the triangular prism element is used as shown in Figure 3.

Illumination Strategy

Choosing a suitable light source is significant because the operating wavelength of the incident light must well balance the sensitivity and the optical nonlinearity. Since the sensitivity and nonlinearity are inversely proportional to the wavelength or proportionally varied with the frequency, the increase in the

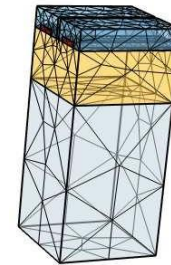


Fig. 3 Mesh on SPR sensor model.

frequency can make the Optical Kerr effect become prominent (Uddin et al., 2020). Thus, it causes significant variations in the refractive index. Therefore, for this study He-Ne laser is used as the light source. He-Ne laser was chosen because it has an operating wavelength of 632.8nm which minimizes the Optical Kerr effect, and it enhanced the sensitivity of the sensor. Based on the operating wavelength, the operating frequency is calculated automatically by the software when the equation is defined as:

$$f = \frac{c}{w} \tag{1}$$

where c is the speed of light and w is the operating wavelength.

Simulation of Delta and Omicron Variants Detection

Different concentrations of spike RBD Delta and Omicron variants were used as shown in Table 3. Based on these concentrations the refractive indices for each concentration were also defined as shown in Table 3. The refractive indices were calculated for each concentration based on Equation (2):

$$n_a = n_o + c_a (dn/dc) \tag{2}$$

where n_a is the refractive index of the virus. In this study, it represented the refractive index of the spike RBD of the Delta and Omicron variants while n_o is the refractive index of the solvent which is a buffer solution that has a refractive index of 1.3348. The c_a is the concentration of the sample and the dn/dc is the refractive increment of the virus that is approximated as 0.181 ml/g (Mostufa et al., 2022).

Simulation of Delta Variant Detection

As the first step, the reactions of spike RBD of the Delta variant (RBDD) binding to the antibody with gold adsorbed (2E8 mAbAu(ads)) to form antibody- antigen complex (RBDD2E8

Table 3. Concentrations and refractive indices of samples

Sample	Concentration [nM] (Ueno <i>et al.</i> , 2022)	Refractive index (Mostufa <i>et al.</i> , 2022)
Spike RBD	0	1.33
Delta variant sample	1.95	1.35
	3.90	1.36
	7.80	1.38
	15.6	1.43
Spike RBD	0	1.33
Omicron variant sample	1.95	1.34
	3.90	1.35
	7.80	1.37
	15.6	1.41

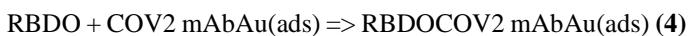
mAbAu(ads)) was defined in the chemistry interface of the COMSOL Multiphysics software and expressed in Equation (3):



The second step was setting the material sweep for Cell 1 and Cell 2 by choosing the sample of the spike RBD of the Delta variant. The material sweep was set because it automatically solves the model for each concentration. Followed by setting the parametric sweeps, which have the range of 64 to 89 degrees for both cells. This range was chosen as it is where the SPR angle shifts were observed. Lastly, the study for Cell 1 and Cell 2 was computed one by one.

Simulation of Omicron Variant Detection

Similarly, the reactions of spike RBD of the Omicron variant (RBDO) binding to the antibody with gold adsorbed (COV2 mAbAu(ads)) to form antibody-antigen complex (COV2 mAbAu(ads)) was defined in the chemistry interface of the COMSOL Multiphysics software as shown in Figure 8 and expressed in Equation (4):



The material sweep for Cell 1 and Cell 2 was set by choosing the sample of spike RBD of the Omicron variant. Followed by setting the parametric sweeps, which have the range of 64 to 89 degrees for both cells. Lastly, the study for Cell 1 and Cell 2 was computed one by one.

RESULTS AND DISCUSSION

Model of the SPR Sensor Based on Kretschmann-Raether Configuration for Delta and Omicron Variants Detection

In this study, the 3D model of the SPR sensor was designed using the COMSOL Multiphysics software. It was performed based on the Kretschmann-Raether configuration that consists of 3 layers. The first layer is the sensing layer that is equipped

with two detecting cells named Cell 1 and Cell 2 as shown in Figure 4.

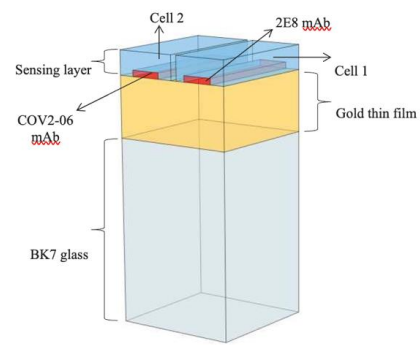


Fig. 4 Antibodies (2E8 mAb and COV2-06) layers in each cell.

The second layer is the Au thin film. Commonly, Au or Ag thin film is preferred to be used for designing the SPR sensor based on the Kretschmann-Raether configuration, but in this study, Au was used because Ag is chemically unstable due to the oxidation that occurs during the chemical interaction (Uddin *et al.*, 2020). Thus, Au thin film was used in this study that involved chemical interaction which is antibody-antigen interactions.

The third layer is the BK7 prism. The BK7 prism was used as it has the highest sensitivity which is 111.11 deg RIU-1 compared to SF10 glass and SF11 glass (Das *et al.*, 2020). According to a study conducted by Das *et al.* (2020), BK7 prism can detect the SARS-CoV-2 spike protein even though a lower concentration of the sample is used. Therefore, BK7 prism was used in this study to detect whether the sample is of the Delta variant or Omicron variant. For the refractive index, Au and BK7 prism had a constant refractive index throughout the study while for the sensing layer the refractive indices of the Cell 1 and Cell 2 were varied depending on the concentrations of the spike RBD of the Delta or Omicron variants that were used during the simulation.

Prior to simulation of the Delta and Omicron variants detection, the 2E8 mAb layer with the concentration of 1.23 nM (Puligedda *et al.*, 2021) and COV2-06 mAb layer with the concentration of 1.74 nM (Mostufa *et al.*, 2021) were added to Cell 1 the Cell 2, respectively as shown in Figure 4. The layers of both monoclonal antibodies were designed based on the physical adsorption, which forms a weak electrostatic bond or permanent covalent bonding by revealing functional groups of easily accessible amino acids. The physical adsorption method was chosen because this method immobilized the antibodies very adjacent to the sensing layer (Sahoo *et al.*, 2016). Thus, this enables the antibody to be easily accessible to interact with the antigen in the detecting cells. In addition, this method also enables the sensor to achieve higher sensitivity (Sahoo *et al.*, 2016).

Simulation of Delta and Omicron Variants Detection

To simulate the detection of the Delta and Omicron variants, He-Ne laser with a wavelength of 632.8 nm was chosen as a light source because it is capable of increasing the sensitivity of the sensor at the same time it minimizes the Kerr effect (Hossain *et*

al., 2019). He-Ne laser was incident at the Au thin film and the sensing layer’s interface. Then different concentrations of spike RBD of the Delta and the Omicron variant were introduced one at a time in both cells as discussed in the following subsections.

Various concentrations of spike RBD proteins of Delta and Omicron variants (0 nM, 1.95 nM, 3.90 nM, 7.80 nM, and 15.6 nM) were used to simulate the detection of the antigen by both Cell 1 and Cell 2 coated antibodies.

Simulation of Delta Variant Detection

The spike RBD Delta variant sample at a concentration of 0 nM was introduced in both Cell 1 and Cell 2 simultaneously. For 0 nM of the spike RBD Delta variant, it only consists of a buffer solution with a refractive index of 1.3348. Therefore, the sample with this concentration used to obtain the SPR angle for Cell 1 and Cell 2, which will act as the reference value to calculate the SPR angle changes that occurred after introducing the spike RBD Delta variant with concentrations of 1.95 nM, 3.90 nM, 7.80 nM and 15.6 nM (Ueno et al., 2022, Mostufa et al., 2021, and Ku et al., 2021).

Once the 0 nM spike RBD Delta variant sample was introduced in both cells, the irradiated light caused the free electrons of the Au thin film to oscillate and absorb the light and caused a sharp decrease in the intensity of the reflected light. This resulted in the reflectivity curve that has a dip known as SPR angle (θ_{SPR}). It was observed that the SPR angles of Cell

1 (θ_{C1SPR}) and Cell 2 (θ_{C2SPR}) are 83.60 degrees and 83.59 degrees respectively (Figure 5). The slight differences between the SPR angles of Cell 1 and Cell 2 for the same concentration of buffer solution were attributed to the variation in the thickness of the Au thin film across the two detecting cells sensing surfaces (Wang et al., 2018).

Upon introduction of the samples in Cell 1, the 2E8 mAb was bound to the spike RBD Delta variant (Puligedda et al., 2021). The binding between the 2E8 mAb and spike RBD Delta variant has increased the refractive index of the sensing layer of Cell 1. This led the SPR angle of Cell 1 to shift from 83.60 degrees to 83.94 degrees as shown in Figure 5. Table 4 shows the SPR angle, SPR angle differences and SPR angle change differences of Cell 1 and Cell 2 for various concentrations of spike RBD Delta protein detection.

There was a slight SPR angle shift from 83.60 degrees to 83.64 degrees when the spike RBD of the Delta variant samples’ concentration varies from 0 nM to 1.95 nM (Table 4). This is because of less amount of spike RBD of the Delta variant present in these lower concentrated solutions to bind to the 2E8 mAb. As a result, fewer antibody-antigen complexes were formed, resulting in small difference in SPR angle. (Moznuzzaman et al., 2021).

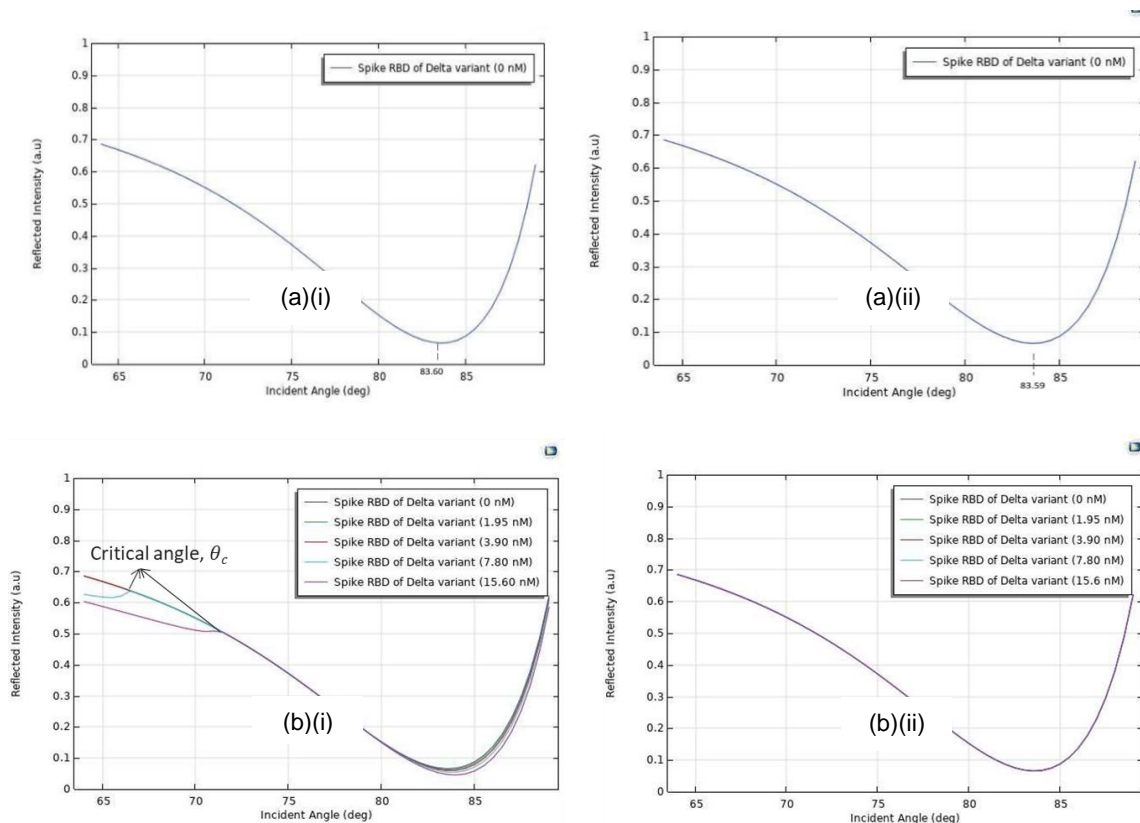


Fig 5. (a) SPR angle of cell when spike RBD Delta variant sample at a concentration of 0 nM introduced at (a)(i) Cell 1 and (a)(ii) Cell 2. **(b)** SPR angle shift occurred after spike RBD Delta variant sample with concentrations of 1.95 nM, 3.90 nM, 7.80 nM, and 15.6 nM were introduced in (b)(i) Cell 1 and (b)(ii) Cell 2.

Table 4. SPR angle, SPR angle differences and SPR angle change differences of Cell 1 and Cell 2 for various concentrations of spike RBD Delta

Concentration of spike RBD Delta variant sample	SPR angle, θ^{C1}_{SPR} [deg]	SPR angle difference between the different concentrations [deg]		SPR angle change, $\Delta\theta^{C1}_{SPR}$ [deg]	
		Cell 1	Cell 2	Cell 1	Cell 2
0 nM	83.60	-	-	Reference value	Reference value
1.95 nM	83.64	0.04	0.00	0.04	0.00
3.90 nM	83.70	0.06	0.00	0.10	0.00
7.80 nM	83.78	0.08	0.00	0.18	0.00
15.6 nM	83.94	0.16	0.00	0.34	0.00

When the concentrations varied from 1.95 nM to 3.90 nM and 3.90 nM to 7.80 nM, the SPR angle shift increased by 0.06 degrees and 0.08 degrees respectively. This is due to the increase in the amount of the spike RBD of the Delta variant that is present in the sample, so more antibody-antigen interactions occurred (Moznuzzaman et al., 2021). As a result, there is an increase in the SPR angle difference between the different concentrations.

On the other hand, there is a significant increase in the SPR angle difference which is 0.16 degrees when the concentration of the spike RBD of the Delta variant varied from 7.80 nM to 15.60 nM. The significant difference is due to more spike RBD Delta bound to the 2E8 mAb, which means more antibody-antigen complexes causing huge difference in the SPR angle (Moznuzzaman et al., 2021).

Based on the SPR angle shift in Table 4, the presence of the spike RBD of the Delta variant in the sample was determined by calculating the minimum threshold value or the smallest change in the SPR angle. The minimum threshold value was calculated based on the SPR angle shift that occurred after introducing the spike RBD of the Delta variant at a concentration of 1.95 nM. Thus, the minimum threshold value of the SPR angle for Cell 1 was calculated using the values obtained from the Table 7 and using the formula as shown below (Mostufa et al., 2021):

$$\theta_{th}(C1)_{SPR} = |\theta_{0\text{ nM}SPR} - \theta_{1.95\text{ nM}SPR}| = 0.04 \text{ degrees} \quad (5)$$

The presence of the spike RBD Delta variant in the sample was detected when the binding occurred between the 2E8 mAb. The resulting SPR angle change ($\Delta\theta^{C1}_{SPR}$) became greater or equal to the minimum threshold value $\theta_{th}(C1)_{SPR}$ which was 0.04 degrees. If there is no binding occurred between the 2E8 mAb and the spike RBD Delta antigen, then the sample is of non-Delta variant $\theta_{th}(C1)_{SPR}$ was greater.

On the other hand, when the same amount spike RBD Delta samples were loaded onto Cell 2, no significant changes were observed. This is due to the absence of antigen-antibody complex. Thus, the refractive index of Cell 2 remained constant and the SPR angles were not shifted.

Simulation of Omicron Variant Detection

To simulate the Omicron variant detection, different concentrations of spike RBD Omicron variant such as 0 nM, 1.95 nM, 3.90 nM, 7.80 nM, and 15.6 nM were introduced one at a time in both Cell 1 and Cell 2 simultaneously.

Spike RBD Omicron variant at a concentration of 0 nM, which consisted of a similar buffer solution as in spike RBD of the Delta variant was used. Thus, the SPR angles for Cell 1 and Cell 2 were like the ones obtained for the spike RBD of the Delta variant sample at a concentration of 0 nM. The SPR angles obtained for both Cell 1 (θ^{C1}_{SPR}) and Cell 2 (θ^{C2}_{SPR}) were 83.60 degrees and 83.59 degrees respectively. This can be seen from Figures 6. These two SPR angles were used as the reference values to the other spike RBD Omicron variant concentrations (Ueno et al., 2022, Mostufa et al., 2021, & Ku et al., 2021).

When the spike RBD Omicron variant sample at concentrations of 1.95 nM, 3.90 nM, 7.80 nM, and 15.6 nM were introduced, one at a time in Cell 1, the SPR angle shifts were not observed as shown in Figure 15. The data were tabulated in Table 5. Table 5 shows that the SPR angles for all the concentrations of the spike RBD Omicron variant sample were maintained at 83.60 degrees. This is because the 2E8 mAb did not bind to the spike RBD Omicron variant as it has N501Y mutation (Puligedda et al., 2021). As a result, there was no formation of the antibody-antigen complexes. Thus, the refractive index of Cell 1 remained constant and the SPR angles were not shifted.

When the spike RBD Omicron samples (1.95 nM, 3.90 nM, 7.80 nM, and 15.6 nM) were introduced in Cell 2 one at a time, the COV2-06 mAb bound to the spike RBD Omicron variant (Ku et al., 2021). The binding between the COV2-06 mAb and spike RBD Omicron caused an increase of the refractive index of the sensing layer of Cell 2. This has resulted in the SPR angle shifting from 83.59 degrees to 83.95 degrees as shown in Figure 6 (b)(ii).

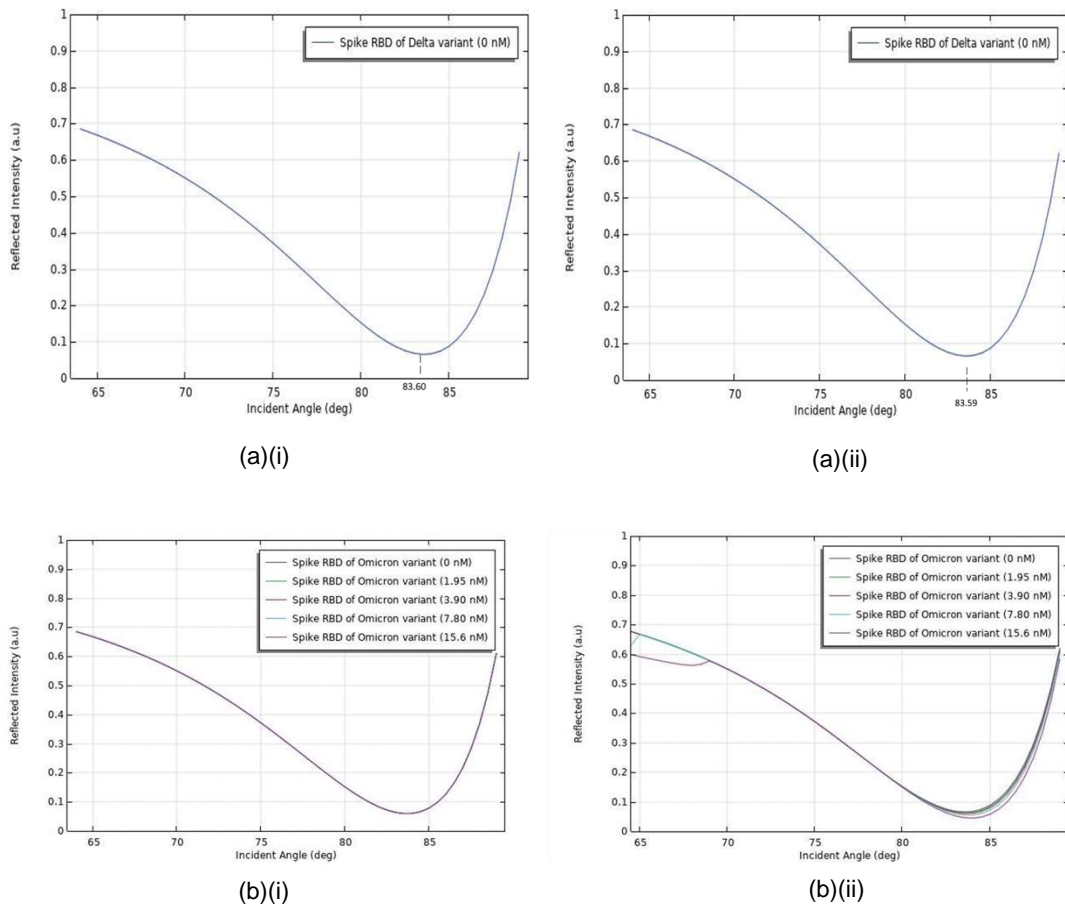


Fig 6. (a) SPR angle of Cell when spike RBD Omicron variant sample at a concentration of 0 nM introduced at (a)(i) Cell 1 and (a)(ii) Cell 2. (b) SPR angle shift occurred after spike RBD of the Omicron variant sample with concentrations of 1.95 nM, 3.90 nM, 7.80 nM, and 15.6 nM were introduced in (b)(i) Cell 1 and (b)(ii) Cell 2.

The SPR angle differences between different concentrations were calculated (Table 5). There was a small SPR angle shift from 83.59 degrees to 83.64 degrees, when a 1.95 nM spike RBD Omicron was loaded. This is because of less amount of spike RBD of the Omicron variant present in these lower

concentrated solutions to bind to the COV2-06 mAb, so fewer antibody-antigen complexes were formed (Moznuzzaman et al., 2021). The SPR angle shift was slightly increasing for 3.90 nM and 7.80 nM spike RBD Omicron loaded on Cell 2. This

Table 5. SPR angle, SPR angle differences and SPR angle change of Cell 1 and Cell 2 for various concentrations of spike RBD Omicron

Concentration of spike RBD Omicron variant sample	SPR angle, θ^{C1}_{SPR} [deg]	SPR angle difference between the different concentrations [deg]		SPR angle change, $\Delta\theta^{C1}_{SPR}$ [deg]	
		Cell 1	Cell 2	Cell 1	Cell 2
0 nM	83.60	-	-	Reference value	Reference value
1.95 nM	83.60	0.00	0.05	0.00	0.05
3.90 nM	83.60	0.00	0.06	0.00	0.11
7.80 nM	83.60	0.00	0.07	0.00	0.18
15.6 nM	83.60	0.00	0.18	0.00	0.36

demonstrated that there was a slight increase in antigen-antibody complex formation (Moznuzzaman *et al.*, 2021).

On the other hand, there was a significant increase in the SPR angle difference which is 0.18 degrees when the concentration of spike RBD of the Omicron variant varies from 7.80 nM to 15.60 nM. The significant difference was due to the higher amount of spike RBD Omicron variant forming complex with COV2-06 mAb (Moznuzzaman *et al.*, 2021).

Similar to the Delta variant detection, the minimum threshold value or the smallest change in SPR angle was calculated based on the SPR angle shift that occurred after introducing the spike RBD of the Omicron variant at a concentration of 1.95 nM (Mostufa *et al.*, 2021). The minimum threshold value of the SPR angle for Cell 2 was calculated using the following formula:

$$\theta_{th}(C2)SPR = |\theta_{0\ nMSPR} - \theta_{01.95\ nMSPR}| = 0.05\ degrees \tag{6}$$

Relationship between SPR Angle Change and Concentration

Linear graphs of SPR angle versus concentration were plotted for Cell 1 and Cell 2 respectively as shown in Figure 7. Both graphs showed the existence of a linear relationship between the concentration and the SPR angle change.

Relationship between SPR Angle and Refractive Index

When graphs were plotted for SPR angle versus the refractive index of the samples in each cell as shown in Figure 8, they showed the existence of a linear relationship between them. This is because when the refractive index of the sample is increased the SPR angle is also increased.

Based on these linear graphs, the sensitivity of the sensor to detect the Delta and Omicron variant was determined by calculating the gradient or by using Equation (3.19) (Mostufa *et al.*, 2021). The sensitivity obtained for Cell 1 is 3.3968 deg RIU⁻¹ while the sensitivity obtained for Cell 2 is 4.5803 deg RIU⁻¹. When comparing the sensitivity of Cell 1 and Cell 2, Cell 2 has a slightly higher sensitivity than Cell 1. This is because in Cell 1 the field energy required for exciting the strong plasmon that is necessary for the sensing could have lost due to the scattering (Bing *et al.*, 2020).

CONCLUSION

In this study, a SPR sensor based on the Kretschmann-Raether configuration was designed with two detecting cells named Cell 1 and Cell 2 using COMSOL Multiphysics software to detect the Delta and Omicron variants respectively. Cell 1 consisted of 2E8 mAb layer while Cell 2 consisted of COV2-06 mAb layer. The detection of the Delta and Omicron variants were simulated

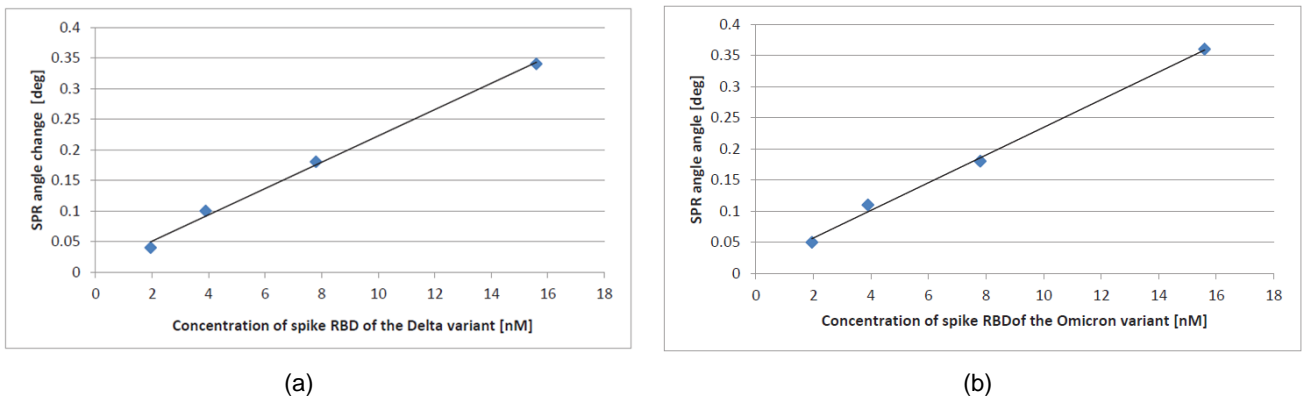


Fig 7. Relationship between the SPR angle change and the concentration of the samples in (a) Cell 1 and (b) Cell 2.

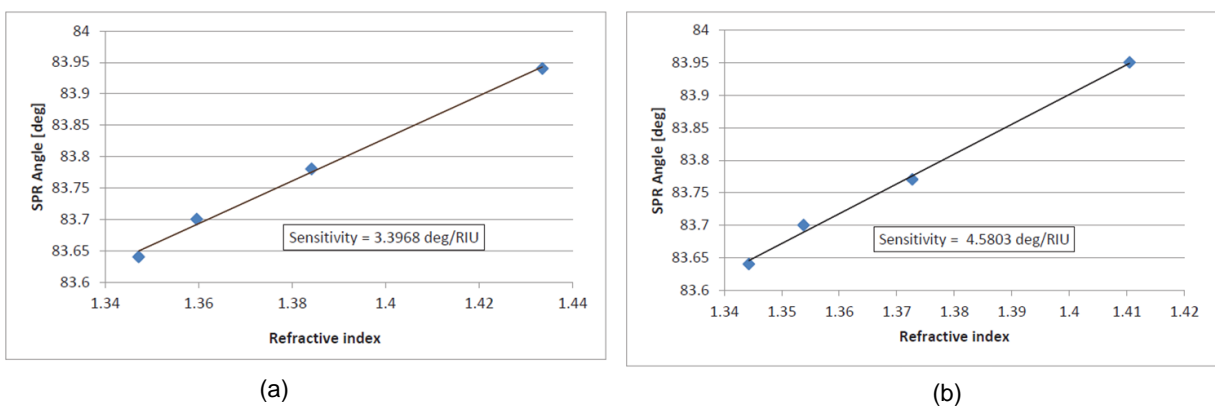


Fig 8. SPR angle versus refractive index of samples in (a) Cell 1 for Delta variant and (b) Cell 2 for Omicron variant.

based on the formation of the antibody-antigen complexes that caused the SPR angle shifts in both Cell 1 and Cell 2. During simulation, the SPR angle shifts were only observed in Cell 1 when different concentrations of the spike RBD of the Delta variant were introduced in both cells. This indicated that the sample is of the Delta variant. Similarly, when different concentrations of the spike RBD of the Omicron variant were introduced in both cells, the SPR angle shifts were only observed in Cell 2 and indicated that the sample is of the Omicron variant. This showed that the designed SPR sensor can distinguish and detect the Delta and Omicron variants successfully based on the antibody-antigen interaction.

Furthermore, there were linear increases observed in the SPR angle changes in both cells when different concentrations of spike RBD of the Delta and Omicron variants were introduced. This showed that the designed SPR sensor has desired characteristic with the sensitivity of $3.3968 \text{ deg RIU}^{-1}$ for Cell 1 and $4.5803 \text{ deg RIU}^{-1}$ for Cell 2. Therefore, the SPR sensor based on the Kretschmann-Raether configuration could be implemented for multiple SARS-CoV-2 variants detection. In addition, it is also a potential alternative tool for currently available multiple SARS-CoV-2 variants detection method that is based on nucleic acid amplification tests as the SPR sensor provides the label-free detection based on the antigen-antibody interactions as shown in this study.

ACKNOWLEDGEMENT

Authors would like to thank UTM Encouragement Research Grant (UTMER) [QJ130000.3851.19J27] from Universiti Teknologi Malaysia (UTM) for financially supporting this study.

REFERENCES

- Asghari, A., Wang, C., Yoo, K. M., Rostamian, A., Xu, X., Shin, J. D., Dalir, H., Chen, R. T. 2021. Fast, accurate, point-of-care COVID-19 pandemic diagnosis enabled through advanced lab-on-chip optical biosensors: Opportunities and challenges. *Applied physics reviews*, 8(3), 03-1313.
- Barrios, C. A. 2022. Modeling of a Graphene Nanoribbon-based Microfluidic Surface Plasmon Resonance Biosensor. *Plasmonics*, 17(2), 745-752.
- Bing, P., Sui, J., Wu, G., Guo, X., Li, Z., Tan, L., Yao, J. 2020. Analysis of dual channel simultaneous detection of photonic crystal fiber sensors. *Plasmonics*, 15(4), 1071-1076.
- Das, C. M., Guo, Y., Yang, G., Kang, L., Xu, G., Ho, H. P., Yong, K. T. 2020. Gold Nanorod Assisted Enhanced Plasmonic Detection Scheme of Covid-19 SARS-Cov-2 spike protein. *Advanced Theory and Simulation*, 3(11), 58-73.
- Dormeny, A. A., Sohi, P. A., Kahrizi, M. 2020. Design and simulation of a refractive index sensor based on SPR and LSPR using gold nanostructures. *Results in Physics*, 16, 102-869.
- Hossain, M. B., Rana, M. M., Abdulrazak, L. F., Mitra, S., & Rahman, M. 2019. Graphene-MoS₂ with TiO₂-SiO₂ layers based surface plasmon resonance biosensor: Numerical development for formalin detection. *Biochemistry and biophysics reports*, 18, 100639.
- Ku, Z., Xie, X., Davidson, E., Ye, X., Su, H., Menachery, V. D., Li, Y., Yuan, Z., Zhang, X., Muruato, A. E., I Escuer, A. G., Tyrell, B., Doolan, K., Doranz, B. J., Wrapp, D., Bates, P. F., McLellan, J. S., Weiss, S. R., Zhang, N., Shi, P. Y., ... An, Z. 2021. Molecular determinants and mechanism for antibody cocktail preventing SARS-CoV-2 escape. *Nature communications*, 12(1), 469.
- Michel, D., Xiao, F., Alameh, K. 2017. A compact, flexible fiber-optic Surface Plasmon Resonance sensor with changeable sensor chips. *Sensors and Actuators B: Chemical*, 246, 258-261.
- Mostufa, S., Akib, T. B. A., Rana, M. M., Mehedi, I. M., Al-Saggaf, U. M., Alsaggaf, A. U., ...Alam, M. S. 2021. Numerical approach to design the graphene-based multilayered surface plasmon resonance biosensor for the rapid detection of the novel coronavirus. *Optics Continuum*, 1(3), 494-515.
- Moznuzzaman, M., Khan, I., Islam, M. R. 2021. Nano-layered surface plasmon resonance-based highly sensitive biosensor for virus detection: A theoretical approach to detect SARS-CoV-2. *AIP advances*, 11(6), 065023.
- Pulgedda, R. D., Al-Saleem, F. H., Wirblich, C., Kattala, C. D., Jović, M., Geiszler, L., Devabhaktuni, H., Feuerstein, G. Z., Schnell, M. J., Sack, M., Livornese, L. L., Jr, Dessain, S. K. 2021. A Strategy to Detect Emerging Non-Delta SARS-CoV-2 Variants with a Monoclonal Antibody Specific for the N501 Spike Residue. *Diagnostics (Basel, Switzerland)*, 11(11), 2092.
- Sahoo, P.R., Swain, P., Nayak, S.M., Bag, S., Mishra, S., R. 2016. Surface plasmon resonance based biosensor: A new platform for rapid diagnosis of livestock diseases. *Vet World*. 9(12):1338-1342.
- Uddin, S. M., Chowdhury, S. S., Kabir, E. 2020. Numerical analysis of highly sensitive Surface Plasmon Resonance for SARS-CoV-2 detection. *Plasmonics (Norwell, Mass.)*. Advance Online Publication, 1-13.
- Ueno, M., Iwata-Yoshikawa, N., Matsunaga, A., Okamura, T., Saito, S., Ashida, S., ... Ishizaka, Y. 2022. Isolation of human monoclonal antibodies with neutralizing activity to a broad spectrum of SARS-CoV-2 viruses including the Omicron variants. *Antiviral Research*, 201, 105297.
- Wang, D. S., Fan, S. K. 2016. Microfluidic Surface Plasmon Resonance Sensors: From Principles to Point-of-Care Applications. *Sensors (Basel, Switzerland)*, 16(8), 1175.
- Wang, D., Loo, F. C., Cong, H., Lin, W., Kong, S. K., Yam, Y., Chen, S. C., Ho, H. P. 2018. Real-time multi-channel SPR sensing based on DMD-enabled angular interrogation. *Optics express*, 26(19), 24627-24636.
- Xi, H., Jiang, H., Juhas, M., Zhang, Y. 2021. Multiplex Biosensing for Simultaneous Detection of Mutations in SARS-CoV-2. *ACS omega*, 6(40), 25846-25859.